Available online at www.sciencedirect.com

ScienceDirect

Procedia Manufacturing 00 (2019) 000–000

Procedia MANUFACTURING

www.elsevier.com/locate/procedia

47th SME North American Manufacturing Research Conference, NAMRC 47, Pennsylvania, USA

Adaptive repair and digitization for hybrid manufacturing

Myong Joon Kim, Maxwell Praniewicz, Thomas R. Kurfess, Christopher Saldana*

George W. Woodruff School of Mechanical Engineering, Georgia Institute of Technology, 801 Ferst Drive, Atlanta, Georgia 30332

* Corresponding author. *E-mail address:* christopher.saldana@me.gatech.edu

Abstract

Repair of aerospace components represents a significant opportunity for hybrid manufacturing systems to reduce high scrap rate through automation of the inspection, additive and subtractive processes. In this study, a series of on-machine profile digitization strategies were investigated to determine the effects on accuracy of non-rigid registration of blade component geometry and downstream quality measures pertaining to parent material blendlines. The profile digitization strategies investigated include dense sampling methods and curvature-based segmentation approaches. A model was developed to predict the accuracy of the digitization approaches and a series of machining tests were also conducted to show the predictive capability of the model. From these results, it is seen that curvature-based segmentation methods provide an accurate and rapid digitization solution for blend-type repairs.

Keywords: hybrid manufacturing, digitization, adaptive repair, remanufacturing

1. Introduction

Repair and remanufacture to extend the life cycle of aerospace parts has been a great interest due to the high cost associated with the of overhaul and new part replacement. Approximately 8% of the operating costs of an airplane are due to jet engine maintenance and 50% of the overhaul costs are due to the costs associated with airfoils [1, 2]. Moreover, the unique repair and alteration required for this class of parts is due to part-specific geometry changes that occur in response to environmental conditions. These part-specific repairs require intensive process planning work, multiple setups between different stations, and skill intensive manual operations including additive manufacturing (AM), subtractive manufacturing (SM), and manual abrasive finishing. To counter the challenge, hybrid manufacturing (HM) intends to combine AM and SM in a single setup to increase manufacturing efficiency. This is automated methods for design and execution of repair process plans that are needed to improve the overall effectiveness of the repair process in terms of time, cost, and quality [3, 4].

An attractive solution to curtail inconsistency in the blade repair process and leverage automation capabilities is to carry out the entirety of the repair-related procedures on a single manufacturing platform in a HM framework. HM-based repair strategies provide advantages for interchange of parts between inspection, subtractive, and additive manufacturing paradigms so to automate repair without the associated challenges of multi-setup registration and digitization in batch processing methods. For example, in Ref. [1] demonstrated capability to integrate SM and AM strategies to remanufacture aerospace turbine blades by probing, welding, and blending of the blade tip. The paper demonstrated adaptive re-tipping of the blade with less than 10μm of mismatch between parent material and the blended region, as well as good fusion of the weld on the parent material. However, this particular work is limited in that: (1) the probing and morphing algorithm used was not applied to inform the welding repair process, (2) the probing and

morphing algorithm utilized was not explicitly explained, and (3) little quantitative analysis was provided to demonstrate ability to repair the blades to meet the quality certification. In this regard, to-date, a complete description of HM-based strategies has been limited, especially in terms of the ability of such methods to carry out adaptive repair for part-specific repair requirements [5, 6, 7].

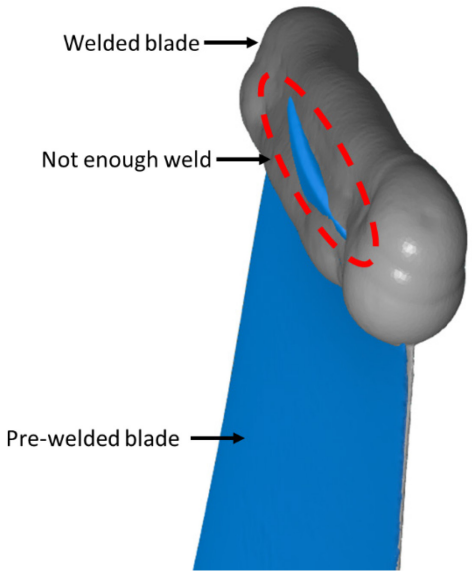

Fig. 1. Structured light scan of pre-welded blade (blue) and post-welded blade (grey). Not enough weld is deposited on convex side of the blade (red dashed oval).

An adaptive geometry transformation introduced in Ref. [8] established a morphing algorithm to non-rigidly register the ideal blade geometry to the deformed blade geometry so to accurately interpolate the tip geometry underneath the weld, which accounts for angular distortion, lean, and wear of the parent blade and to mitigate inconsistency in fixturing. Morphological deformation of the serviceable blade is important in adaptive hybrid blade repair because each blade exhibits unique deformation after it is extracted from service. Further, the accuracy of registration determines the final repaired product. In the additive process, the registered 3D tip geometry provides a template to guide the additive toolpath to not only increase material efficiency, but also prevent the problem of having insufficient weld to carry out the repair, as in Fig. 1. Once the tip is welded, machining is used to blend the weld to the parent material, with the ideal result being kept within the specified limit suited to customer requirement [9].. While this method was successful in adaptive repair of the blade geometries, it did not consider the required digitization of the blade model as well as optimization of probing and geometric reconstruction strategies to guide the repair process.

The present study establishes an optimized probing strategy to implement in a HM-based repair process so to generate cross-section profiles for reconstructing the 3D blade geometry. To understand the impact of these probing strategies, both simulated and experimental blending tests were carried out and quality of the blend was evaluated so to characterize surface profile deviations and step size deviations in the transition region between the machined and parent surfaces. This region where the material transitions between the machined and parent surfaces is defined as the blendline.

Nomenclature

Zn	horizontal 2D blade profile
N	number of 2D profiles along the entire blade
Nnom_zi	2D profiles on nominal blade
Ndef_zi	2D profiles on deformed blade
W	number of profiles in the weld height
S	number of segments in 2D profile
P	number of points in one segment of 2D profile
H	order of fitted polynomial on thickness distribution

2. Method

The adaptive repair process requires integrated inspection, additive, and subtractive processing to achieve a blendline target specification for a serviced blade geometry. The entire digitization and registration strategy for an automated blending operation is depicted as a flow chart in Fig 2. In this approach, digitization of the blade geometry is needed to facilitate non-rigid registration. The target condition needed is that which achieves a sufficient target profile reconstruction specification while also limiting the number of points required, thereby reducing processing time.

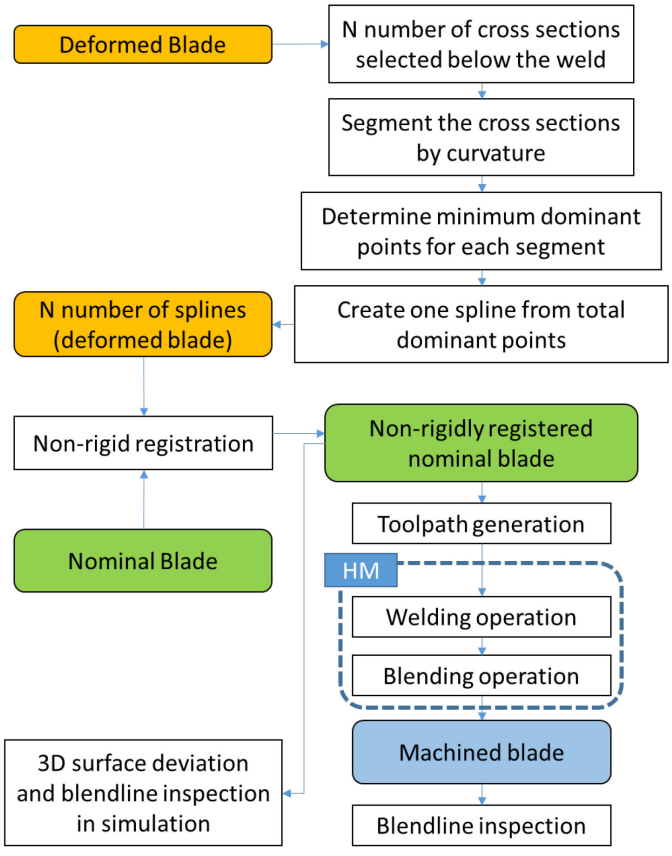

Fig. 2. Overall strategy of digitization of the deformed blade and registration of the nominal blade for blending operation and inspection.

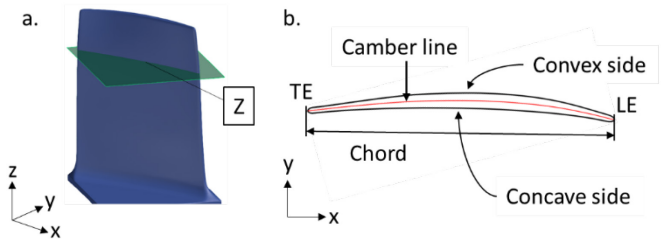

Fig. 3. Basic airfoil profile. (a) Nominal model of 3D airfoil geometry and z-axis cross sectional plane (green) at the inspection height. (b) Camber line, chord, leading edge (LE), trailing edge (TE), convex and concave side of the airfoil is depicted at section Z.

To validate the strategy, several sets of nominal blade geometry and deformed blade geometry were generated considering basic airfoil geometry as in Fig. 3. The original blade geometry (Fig. 4a) and that of the as-received deformed blade geometry were analyzed to determine the profile deviation that are shown in the used blades (Fig. 4b). In this regard, the nominal blade geometry was sectioned with N planes perpendicular to the blade stacking axis (shown as the Z axis), this creating 2D cross-sectional blade profiles to assess the trend in twist/angular change and chord length deviation, as in Fig. 4c and Fig. 4d. Among these N profiles, W indicates the number of 2D blade profiles of the nominal blade in the weld region and used to register the nominal blade to the deformed blade for interpolating the tip geometry. The surrogate blades are digitized using (N-W) cross-sectional profiles in the non-weld region.

For the probing strategies employed in the present study, the minimum number of dominant points on the 2-D cross-sectional contours are determined so to regenerate the profile within an acceptable tolerance. In finding the minimum number of dominant points of the contour, different methods were compared relative to the maximum profile deviation, total profile deviation, and average profile deviation. After profile digitization, the target blade tip geometry (e.g., in the weld region) of the deformed blade is determined by interpolation of the morphed nominal blade geometry. The toolpath for the blending operation was derived based on the geometry of the morphed nominal blade. Surface deviation and blendline height analysis as a function of the probing strategy used was determined based on simulation as well as experimental machining tests.

2.1. Parametric design of surrogate blade

A representative blade geometry was designed based on that of an actual aeroengine compressor blade so to simulate similar features of the part for accurate representation. Twist angle, chord length, camber line, and profile thickness distribution data were extracted from multiple horizontal cross sections along the stacking axis. This surrogate blade model does not fully entail the complexity of the original blade; however, it is useful in investigating the effect of the proposed probing methods as it simplifies the required inspection. The surrogate blade was created based on parameters and design intent of the original compressor blade model and is shown in Fig. 5. Blade cross sections along the stacking axis can be determined by either definition of curves of the concave and convex blade surfaces or by determining a profile mean camber line and applying a thickness distribution [10]. Though the first method provides curvature continuity and reduced number of design parameters, the second method ensures more accurate geometric features that are directly linked to blade geometry.

Ten blades which had been used in service where measured at a pre-determined height along the stacking axis to quantify the range of angular and chordal deviations which occur in normal use. The maximum observed deviations in each of these blades were then averaged. The maximum deviation of the deformed blade against the nominal blade is D_{max} at a constant height along the Z-stacking axis as in Fig. 5b. The angular distortion is defined as θ and is due to twist of the profile along the stacking axis. Chordal deviations are defined by D_{tip} due to the erosion in the trailing and the leading edge.

For the purpose of profile digitization for an unknown blade geometry, the mean camber line can be extracted from analysis of experimentally-obtained measurements or digitally-sampled model points from the blade profile. These profile measurements or samples define the profile geometry, where the thickness distribution defines the concave and convex surfaces of the blade [11]. The leading and trailing edges are determined by fitting circles with centers at the extents of the mean camber line and with radius of the leading and trailing edge thickness at that point. The radius and profile edge

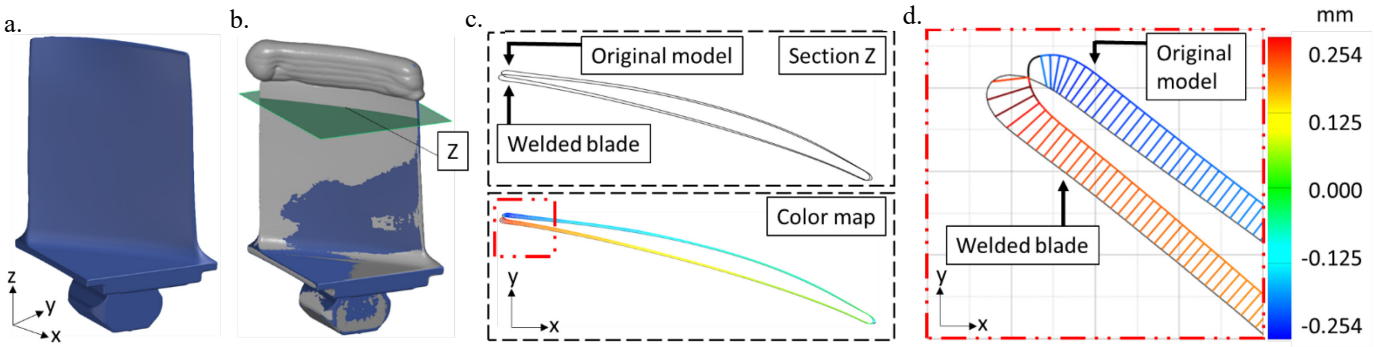

Fig. 4. Images of compressor blades and cross-sectional inspection at probing height. (a) Scan of original model of a pre-weld blade geometry and (b) post-weld blade scan (grey) overlapped on the original model. (c) Cross section at Z height showing slight deviation of two models, and their deviation shown in colormap. (d) Zoom-in of red dotted box.

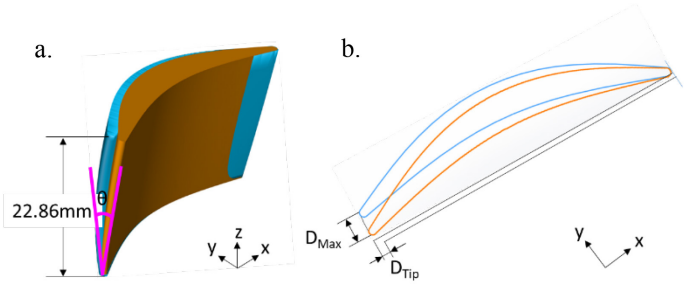

Fig. 5. Designing a nominal and a deformed surrogate blade. The maximum linear deviation and angular distortion of two models are based on inspection on the actual blade scans. (a) The nominal blade (blue) is overlapped to the deformed blade (orange). The top 7.62 mm of the industrial blade, which is the only part that is serviceable, is scaled up by three times. (b) Maximum deviation (D_{max} =0.762mm) and the angular distortion (θ = 1.91 deg.) are also scaled up for machinability and visualization purposes.

thickness on both edges, maximum thickness, chord length and chord angle between two different cross sections are extracted from the original blade profile. The parameters are used as threshold to determine the accuracy of the cross sections which then be lofted to create 3D model.

2.2. Curvature-based sectioning for profile digitization

A curvature-based sectioning (CBS) approach was developed to facilitate profile digitization and is shown in Fig. 6. In this approach, N cross-sectional profiles in the non-repair region are divided into segments based on curvature. Curvature is calculated by taking the second derivative at each point of the profile. A 15th order one-dimensional median filter is applied to the curvature values, and the values are plotted against the position along the profile. A threshold is then applied to split the profile into segments such that each segment can be represented with one spline consisting of less than 7 points and 12.7μm deviation. Once the profile is split into S total segments, three points are evenly distributed on the segment and a curve is reconstructed using cubic spline interpolation. If recreated curves exceeded the 12.7μm tolerance from the respective original segment, additional points are added and redistributed. This iterative cycle continues until P points are determined to recreate a spline that would fit the original segment within the tolerance specification. Each of the S segments goes through this same process to find the minimum number of points to recreate the entire profile. This CBS approach allows for reduction in number of points based on local curvature and in the present study this was compared with a dense sampling (DS) approach based on equidistant but high resolution sampling of the profile geometry.

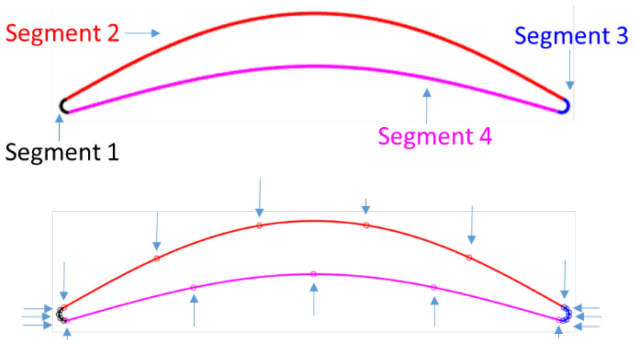

Fig. 6. Illustration of segmented cross-sectional profile and dominant points to recreate each segment. The 2D contour is divided into four segments (a). Minimum number of dominant points and their positions are determined on each segment to recreate them within 12.7 of tolerance (b).

2.3. Non-rigid registration for adaptive HM-based repair

After profile digitization, the measured or sampled profile is used to non-rigidly register the nominal blade geometry to accurately predict the tip geometry of the blade using the method described in Ref. [8]. In this approach, for each individual 2-D profile, a camber line is calculated by a profile mean line method, where the camber line is the set of all center points of the largest circles that can be inscribed with the 2D blade profile in the corresponding plane that is perpendicular to the stacking axis of the blade. The ends of this camber are then limited to center point of the inscribed circle at the leading and trailing edges. When the camber line is fully defined, the profile thickness distribution (TD) about the line is calculated by fitting an Hth order polynomial to a set of the normal distances from the camber line to the profile. The order of polynomial is determined iteratively until the polynomial fits the given set of distance with fitting polynomial regression R^2=1.

The nominal blade geometry is non-rigidly registered to the deformed blade geometry so to adapt the blade tip geometry in the non-repair region. The inputs for the non-rigid registration are Nnom_zi, TDnom_zi, Ndef_zj, and TDdef_zj, and the outputs are Nreg_zi. Nnom_zi is the number of 2D cross-sectional profiles of the nominal blade at zi height ($1 \le i \le K$, where i and K are integer), and TDnom_zj is the thickness distribution corresponding to the profile at zi height. Ndef_zj is the number of 2D cross-sectional profiles of the deformed blade that accounts for intentionally introduced lean and twist at zj height ($1 \le j \le L < K$, where j, L, K are integer, and zL is the greatest z height below the weld), and TDdef_zj is the thickness distribution corresponding to the profile at zj height. The information of the two geometry is used to non-rigid registration which consists of rigid registration, non-rigid transformation, and registered profile (Nreg_zi) creation.

3. Results

The nominal surrogate blade geometry was used to validate the effect of digitization approaches (e.g., CBS, DS) on accuracy of non-rigid registration. The cross-sectional profiles in the non-repair region of the deformed blade were digitized and used to non-rigidly register the nominal blade to the deformed blade. The final registered blade geometry was then used to create machining toolpaths for remanufacture of the blade geometry. In the case of surface deviation between the deformed blade and the final registered blade, quality defects would result as this deviation would create a measurable blendline step and/or profile thickness deviation. The relative differences in probe-based inspection time using a Renishaw RMP600 high accuracy machine probe were calculated to be 15 minutes for the DS method and 30 seconds for the CBS method.

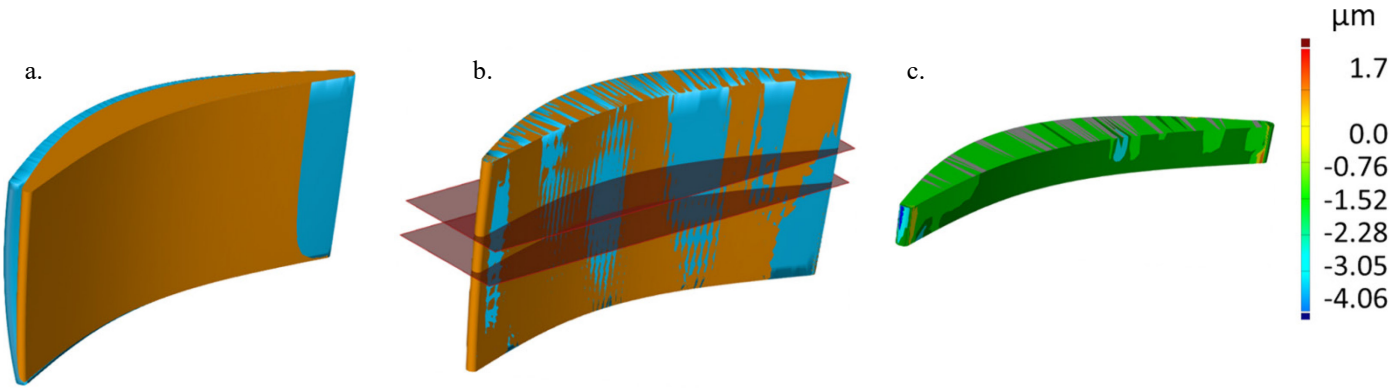

Fig. 7. The nominal blade has been registered to the deformed model and the surface deviation is analyzed. (a) Deformed blade(orange) is overlaid on the non-registered nominal blade (blue). (b) Nominal blade is registered to the deformed blade and two horizontal planes are drawn to set lower and upper boundary of the area where blendline is most likely to exist. (c) The blend line volume is isolated and surface deviation is inspected between deformed blade and registered nominal blade.

Blade cross-section profiles (Zn, maximum height of Zn < 10.44mm, n >= 2) of the deformed blade in the non-repair region were digitized using the CBS and DS digitization approaches. A representative profile deviation is shown in Fig. 7 and the resulting profile deviations are tabulated for the two approaches in Table 1 using normal vectors from the horizontal 2D profile, Zn, towards the digitized profile. The blendline region is defined as 10.44mm≤ z height ≤ 14.25mm (Fig. 7b) which was referenced to the z height of where the bottom of the repair region and non-repair regions intersect and where blendline defects are most likely to occur. From the table, the digitized blade profile that was created using the DS method resulted in significantly smaller profile deviation of 0.6µm compared to that of the CBS method, which resulted in a profile deviation of 86µm. The corresponding 3D surface deviations for these methods were 4µm for the DS method and 109µm in the CBS method. The maximum and average deviations that occur in two different digitizing methods between deformed 2D blade profile and registered 2D blade profiles are recorded in Table 1. Also, the maximum surface deviations and range of deviations between the deformed 3D blade surface and registered 3D blade surface in the blendline region (Fig. 7c) are recorded in the same table.

The surface deviation distribution in the blendline region was analyzed and is shown in Fig. 8. Positive surface deviations (red color in the error bar) indicate unmachined material remaining, and negative surface deviations indicate machining the parent material. For the DS-based digitization approach, maximum surface deviation of 4µm for the blade profile occurred on the concave side of the blade. In comparison, the CBS-based approach resulted in a maximum surface deviation of 109µm on the convex side of the blade profile. From the figure, the surface deviation exhibits a periodic deviation on the blade surface for both digitization approaches.

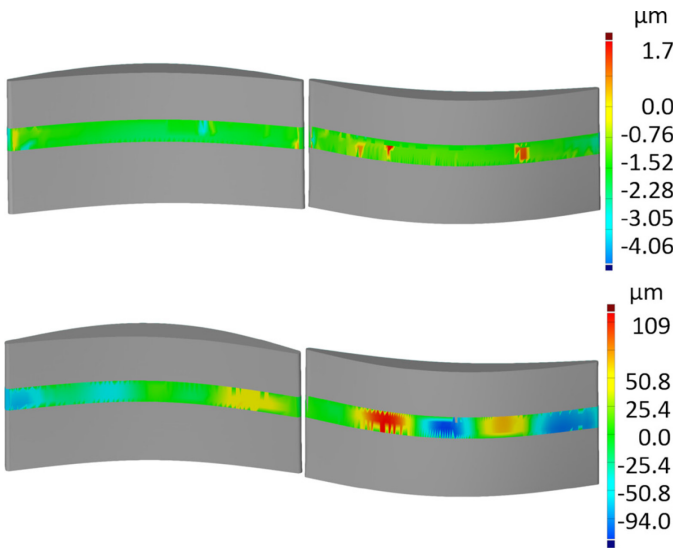

Figure 8. Surface deviation in the blendline region is inspected on the deformed model against non-rigidly registered model. The surface deviation results using (a) dense sampling digitization method and (b) curvature-based segmentation method. Concave and convex side of the models are depicted on the left and right, respectively.

4. Discussion

To explore the capability of the simulation approach to predict the surface deviation and blendline geometry, a series of 5-axis machining tests were carried out using the DS and CBS profile digitization approaches. A Mazak VCU500 machining center was utilized to machine surrogate weld geometries in Al6061-T6 workpieces with 9.525mm diameter 6 flute solid carbide end mill and 4.7625mm diameter 6 flute solid carbide tapered ball end mill. First, the surrogate geometry was machined from billet stock. The blade geometry was then digitized using the CBS and DS approaches and toolpaths were generated based on the non-rigidly registered blade geometry. The blades were fabricated and finish-blended on a single machine setup so to eliminate registration errors in the machining process. In this regard, any profile deviations or

Table 1. 2D profiles and 3D surfaces deviation analysis for two methods

Method	Dominant points	Dev. in 2D profile (µm)		Surface dev. in 3D models (µm)	
		Max. dev	Avg. dev	Max. surface dev	Range of dev
DS	1047	0.6	0.025	4	-4.1 ~ 2
CBS	21	86	28	109	-94 ~ 109

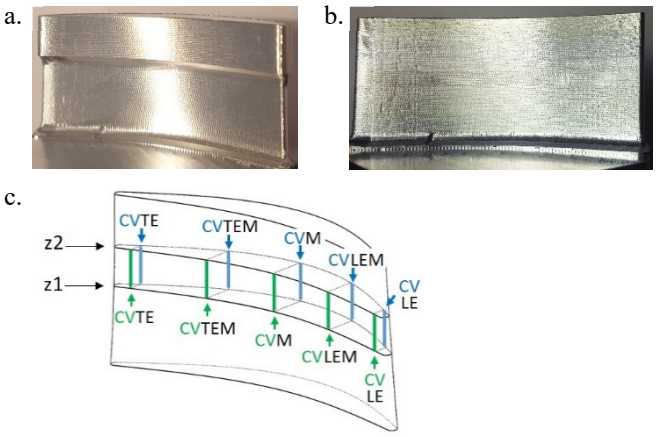

Figure 9. (a) Surrogate welded blade machined in aluminium, and (b) a machined blade using dense sampling method. (c) CMM probing path along the blendline region where CC: Concave, CV: Convex, LE: Leading edge, M: Middle, TE: Trailing edge, LEM: In the middle of LE and M, TEM: In the middle of M and TE.

blendline defects would be due to the digitization approach and physical response during machining. Figure 9 shows the machined geometries for the surrogate welded and finish blended blades, as well as the inspection method used to determine the blendline step geometry.

CMM inspection paths were equidistantly distributed on the concave and convex side to capture effects across the profile of the blade geometry. Each position was inspected starting from a height of z1 = 10.44mm to z2 = 14.25mm, as indicated in Fig. 9c. For this purpose, a Zeiss Micura CMM with a probe stylus ball tip radius of 0.762mm, scanning speed 1.27mm/second, and measurement spacing of 25.4µm was used. The CMM has 0.1µm resolution and scanning error of 0.9µm.

The representative blendline inspection results are shown in Fig. 10a. The measured maximum surface deviation for the DS and CBS methods was 10µm and 104µm, respectively. Further, these measured surface deviations differed from the simulated values by approximately 5µm, which would be due to physical characteristics of the machining process and/or machine alignment errors. It should be noted that visible inspections fail to detect blendline defects smaller than 25.4µm in height, so no blendline was optically observed from the machined part that was created using the DS method.

From these results, the model developed to simulate blendline defect geometry based on profile digitization approaches is accurate and can be used to determine optimal digitization approaches that balance quality requirements with time required to probe the part geometry using on-machine probing. In this regard, one can optimize the profile digitization method with more points at appropriate positions to reduce maximum profile deviation resulting from non-rigid registration.

The optimized digitization method can also be used to guide an adaptive additive manufacturing toolpath, as suggested in Ref. [8]. In a non-adaptive additive repair, the deposited material in the blade tip would have to accommodate the range of blade deformation conditions and result in an unnecessarily larger profile thickness, resulting in process inefficiency due to increased deposition time, increased machining time, material waste, and potentially lower tool life. Integration of these additive, subtractive and inspection procedures within an HM-based repair framework will provide for significant capabilities in this regard.

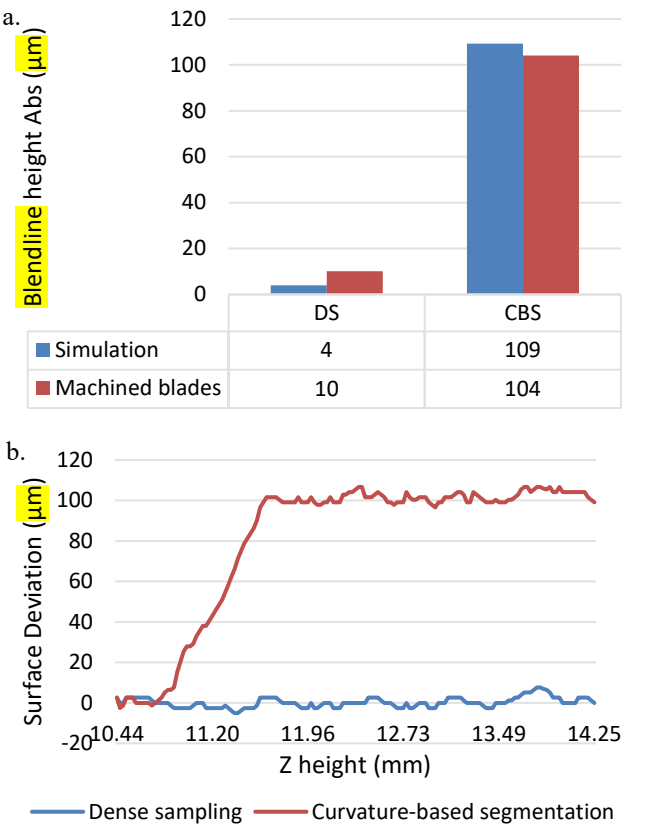

Figure 10. (a) Surface deviation along CMM path against Z height of the blade, (b) absolute value of blendline height observed in simulation compared against CMM results in machined blades.

5. Conclusion

Two methods of digitizing 2D airfoil blade profiles were developed and their effects on 3D non-rigid registration was investigated in simulation and experimental machining tests. A dense sampling method was shown to be capable of accurately recreating 2D profile and registering 3D blade tip geometry. A curvature-based segmentation method was also used and was shown to result in lower profile accuracy than the dense sampling method. The experimental results were found to agree with the simulation predictions. The capabilities of this model to guide selection of effective profile digitization approaches for HM-based repair were also discussed. Future work will pursue further optimization of digitization methods on a wide range of surrogate blade geometries, as well as thorough analysis on blendline region.

Acknowledgements

The authors would like to acknowledge partial support from the National Physical Sciences Consortium (NPSC) for fellowship support for M. Praniewicz. This work was also partially supported by NSF CMMI-1646013, CMMI-1825640 and IIP-1631803.

References

[1] Jones, J. B., McNutt, P., Tosi, R., Perry, C., & Wimpenny, D. I. (2012). Remanufacture of turbine blades by laser cladding, machining and in-process scanning in a single machine.

[2] Aschenbruck, J., R. Adamczuk, and J.R. Seume, Recent Progress in Turbine Blade and Compressor Blisk Regeneration. Procedia CIRP, 2014. 22: p. 256-262.

[3] Kerr, W., & Ryan, C. (2001). Eco-efficiency gains from remanufacturing: A case study of photocopier remanufacturing at Fuji Xerox Australia. Journal of cleaner production, 9(1), 75-81.

[4] R. Steinhilper, Recent trends and benefits of remanufacturing: from closed loop businesses to synergetic networks, in: Environmentally Conscious Design and Inverse Manufacturing, 2001. Proceedings EcoDesign 2001: Second International Symposium on, 2001, pp. 481-488.

[5] Yilmaz, O., Noble, D., Gindy, N. N., & Gao, J. (2005). A study of turbomachinery components machining and repairing methodologies. Aircraft Engineering and Aerospace Technology, 77(6), 455-466.

[6] Rong, Y., Xu, J., & Sun, Y. (2014). A surface reconstruction strategy based on deformable template for repairing damaged turbine blades. Proceedings of the Institution of Mechanical Engineers, Part G: Journal of Aerospace Engineering, 228(12), 2358-2370.

[7] Nagel, J. K., & Liou, F. W. (2012). Hybrid manufacturing system modeling and development. Paper presented at the ASME 2012 International Design Engineering Technical Conferences and Computers and Information in Engineering Conference.

[8] Praniewicz, M., Kurfess, T., & Saldana, C. (2018). An Adaptive Geometry Transformation and Repair Method for Hybrid Manufacturing. Journal of Manufacturing Science and Engineering, 141(1), 011006-011006-011008. doi:10.1115/1.4041570

[9] Gao, J., Folkes, J., Yilmaz, O., & Gindy, N. (2005). Investigation of a 3D non‐contact measurement based blade repair integration system. Aircraft Engineering and Aerospace Technology, 77(1), 34-41. doi:doi:10.1108/00022660510576028

[10] Ferrando, L., Kueny, J.-L., Avellan, F., Pedretti, C., & Tomas, L. (2004). Surface parameterization of a Francis runner turbine for optimum design. Paper presented at the 22nd IAHR Symposium on hydraulic machinery and systems.

[11] Koini, G. N., Sarakinos, S. S., & Nikolos, I. K. (2009). A software tool for parametric design of turbomachinery blades. Advances in Engineering Software, 40(1), 41-51.

[12] Ding, D., Pan, Z., Cuiuri, D., & Li, H. (2015). Wire-feed additive manufacturing of metal components: technologies, developments and future interests. The International Journal of Advanced Manufacturing Technology, 81(1-4), 465-481.